

## Ab Initio and DFT Potential Energy Surfaces for Cyanuric Chloride Reactions

Sharmila V. Pai,<sup>†</sup> Cary F. Chabalowski, and Betsy M. Rice\*

U.S. Army Research Laboratory, Aberdeen Proving Ground, Maryland 21005-5066

Received: December 17, 1996; In Final Form: March 5, 1997<sup>⊗</sup>

*Ab initio* and nonlocal density functional theory (DFT) calculations were performed to determine reaction mechanisms for formation of the six-membered ring  $C_3N_3Cl_3$  (cyanuric chloride) from the monomer cyanogen chloride (CICN). MP2 geometry optimizations followed by QCISD(T) energy refinements and corrections for zero-point energies for critical points on the potential energy surface were calculated using the 6-31G\* and 6-311+G\* basis sets. DFT (B3LYP) geometry optimizations and zero-point corrections for critical points on the potential energy surface were calculated with the 6-31G\*, 6-311+G\*, and cc-pVTZ basis sets. Good agreement is found for MP2 and DFT geometries and frequencies of cyanuric chloride and CICN when compared with experimental values. Two formation mechanisms of cyanuric chloride were investigated, the concerted triple association ( $3 \text{ CICN} \rightarrow \text{cyanuric chloride}$ ) and the stepwise association ( $3 \text{ CICN} \rightarrow \text{Cl}_2\text{C}_2\text{N}_2 + \text{CICN} \rightarrow \text{cyanuric chloride}$ ). All calculations show that the lower energy path to formation of cyanuric chloride is the concerted triple-association. MP2 and DFT intrinsic reaction coordinate calculations starting from the transition state for concerted triple association reaction proceeding toward the isolated monomer resulted in the location of a local minimum, stable by as much as 8.0 kcal/mol, that corresponds to a weakly-bound cyclic  $(\text{CICN})_3$  cluster. The existence of this cluster on the reaction path for the concerted triple association could lower the entropic hindrance to this unusual association reaction mechanism. The DFT/cc-pVTZ barrier to concerted triple association relative to isolated CICN is 42.9 kcal/mol. The QCISD(T)/MP2/6-311+G\* barrier to concerted triple association is 41.0 kcal/mol. The DFT/cc-pVTZ barrier to formation of the dimer (stepwise association reaction) is 63.4 kcal/mol while the QCISD(T)/MP2/6-311+G\* barrier is 76.7 kcal/mol. The barrier to formation of cyanuric chloride relative to the  $(\text{CICN})_3$  minimum requires  $\sim 46$ – $49$  kcal/mol, indicating that the concerted triple-association reaction *via* formation of the  $(\text{CICN})_3$  prereaction intermediate is the lower energy path to formation of cyanuric chloride. The temperature-corrected ( $T = 298$  K) heats of reaction for formation of cyanuric chloride from CICN are  $-63.4$  and  $-61.2$  kcal/mol for the B3LYP/cc-pVTZ and the QCISD(T)/MP2/6-311+G\* predictions, respectively.

### I. Introduction

CICN and HCN-containing munitions were mass-produced in the earlier part of this century. It is expected that aged CICN- and HCN-filled munitions will be uncovered in old disposal sites that are being excavated for environmental clean up. These cyanide compounds are extremely toxic and must be destroyed. However, there are reports that CICN and HCN can undergo violent reactions and that cylinders containing these agents explode.<sup>1</sup> It is crucial that the chemistry behind the initiation of these violent events be characterized before handling these munitions as part of an environmental cleanup.

Although little is known about the details of the reactions, it is well known that CICN and HCN will polymerize after long periods of containment.<sup>2</sup> The primary polymerization product of HCN is the cyclic trimer, *sym*-triazine. CICN polymerizes to cyanuric chloride, the chlorinated analog of *sym*-triazine, as well as to other products, including a tetramer of CICN.<sup>3</sup> The slow thermal polymerization of HCN to *sym*-triazine is exothermic and the reaction can be accelerated if the system should reach 184 °C.<sup>4</sup> Since the CICN and HCN systems are similar, explosions of containers of CICN have been attributed to acceleration of the polymerization reaction,<sup>1</sup> although this has not been proven. Our goals are to determine the low-energy reaction mechanism for the formation of the cyclic trimer from isolated monomer and to quantify the energy release. This

information could help determine if the acceleration of the polymerization reactions plays a role in the observed explosions of cylinders containing this agent. Toward this end, we have performed quantum mechanical calculations to characterize the formation of the cyanuric chloride from isolated monomer.

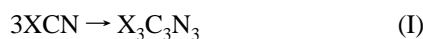
This is the third of our investigations of polymerization reactions of XCN (where X = Cl or H) to the cyclic trimer  $X_3C_3N_3$ . The earlier investigations of the formation reactions of *sym*-triazine from HCN provided information about reaction mechanisms and energetics.<sup>5,6</sup> Additionally, this system was used to assess the performance of density functional theory (DFT) in comparison with QCISD(T) and MP2 predictions of critical points and reaction path properties.<sup>6</sup> In the current study, we are unable to perform MP2 and QCISD(T) calculations using the largest basis set from the previous study,<sup>5,6</sup> cc-pVTZ. However, we are able to perform the same level of DFT calculations for the cyanuric chloride system as in the *sym*-triazine study. Therefore, we undertook the detailed comparison between DFT and *ab initio* for the *sym*-triazine system in anticipation of using the large basis set at the DFT level for the cyanuric chloride system. The results of the comparative study using the large basis set established that the B3LYP results are as good (or better) predictors of energies and properties of critical points along the reaction path for the formation of *sym*-triazine as QCISD(T)/MP2. Therefore, we assume that DFT will treat the chlorinated analog of the *sym*-triazine system with similar accuracy.

The two mechanisms that we assume for the association of XCN to form  $X_3C_3N_3$  are (a) a concerted triple association

<sup>†</sup> National Research Council Postdoctoral Fellow at the U.S. Army Research Laboratory.

<sup>⊗</sup> Abstract published in *Advance ACS Abstracts*, April 15, 1997.

reaction where three XCN molecules come together in a concerted manner to form the cyclic trimer;



and (b) a stepwise addition mechanism where two XCN molecules first come together to form a dimer, followed by a third monomer which adds to the dimer to form  $\text{X}_3\text{C}_3\text{N}_3$ ;



In this study, we will characterize the trimerization reactions of ClCN assuming reactions I and II above. Although there are no data available to shed light on the mechanisms of cyanuric chloride reactions, vibrational and structural data of cyanuric chloride are available and will allow us to further calibrate our theoretical methods through comparison with experiment. We present both *ab initio* [QCISD(T) and MP2] and nonlocal density functional theory calculations for critical points on the potential energy surface for formation reactions of cyanuric chloride.

## II. Methods

All calculations reported herein were performed using the Gaussian 94 set of programs.<sup>7</sup> Structures of critical points were located through geometry optimizations at the MP2 and DFT levels using the 6-31G\*<sup>8</sup> and 6-311+G\*<sup>9</sup> basis sets. Also, DFT geometry optimizations using the cc-pVTZ basis set<sup>10</sup> were performed for all critical points on the potential energy surface (PES). All critical points were characterized through normal mode analyses. Subsequent QCISD(T) energy refinements on the MP2-optimized structures were performed. The DFT calculations used the Gaussian 94 implementation of Becke's three-term hybrid functional (B3)<sup>11</sup> and the Lee, Yang, and Parr (LYP)<sup>12</sup> correlation functional with nonlocal corrections to both the exchange and correlation functionals. The resulting exchange-correlation functionals are referred to in the text as B3LYP. All geometry optimizations met the default convergence criteria given by Gaussian 94.<sup>7</sup> All DFT calculations were performed using the default grid size given in Gaussian 94.<sup>7</sup> Intrinsic reaction coordinate (IRC) calculations leading from the transition states for (I) and (II) were performed to establish reaction paths. The IRC calculations were performed using the 6-31G\* basis set at both the MP2 and DFT levels. The IRC calculations were terminated only when minima were reached as defined by the default convergence criteria of the Gaussian 94 set of programs.<sup>7</sup>

## III. Results and Discussion

Molecular structures for critical points corresponding to reactions I and II are shown in Figure 1. Table 1 lists the geometric parameters of these critical points. The atom labels in Table 1 are consistent with the labeling on the structures shown in Figure 1. In the following comparisons of calculated structures and frequencies with experiment, we will assume that the most accurate *ab initio* and DFT predictions correspond to the largest basis set used at each level, *i.e.*, the MP2/6-311+G\* and DFT/cc-pVTZ results, respectively. MP2 and DFT predictions using smaller basis sets than these are provided in the tables to show basis set dependencies, but they will not be discussed in detail nor compared with experiment.

**Geometries:** Structural data for gas-phase cyanuric chloride are not available; the only experimental information about the molecular structure of cyanuric chloride comes from electron<sup>13</sup> and X-ray diffraction studies<sup>14-16</sup> of the crystal. The X-ray analysis of the cyanuric chloride crystal by Pascal and Ho<sup>14</sup>

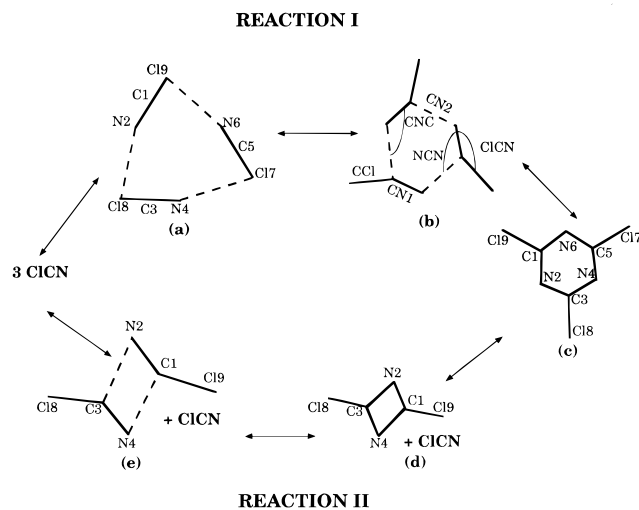


**Figure 1.** Structures of (a) the hydrogen-bonded (ClCN)<sub>3</sub> cluster located on the concerted triple-association path, (b) transition state for the concerted triple-association reaction (reaction I), (c) cyanuric chloride, (d) the stable dimer species Cl<sub>2</sub>C<sub>2</sub>N<sub>2</sub> associated with the stepwise association mechanism (reaction II) and, (e) the transition state to the stepwise formation of the dimer from ClCN (reaction II). All structures except (e) are planar. Atom labels in (a) and (c) are consistent with labels in Table 1.

indicate that the molecular geometry has approximate  $D_{3h}$  symmetry and that the triazine ring is planar and consists of equilateral C–N bonds (1.325 Å). The triazine ring is not a regular hexagon; the N–C–N and C–N–C angles are reported to be 127.4° and 112.7°, respectively. These structural parameters are very similar to those of gaseous *sym*-triazine.<sup>18</sup> Pascal and Ho<sup>14</sup> did not report the C–Cl bond distance. Another X-ray diffraction study by Maginn *et al.*<sup>16</sup> provided a mean C–Cl intramolecular bond distance of 1.703 Å and a mean observed NCN angle of 126.23°, which differs by 1.2° from that observed by Pascal and Ho.<sup>14</sup> An earlier electron diffraction study of the crystal<sup>13</sup> provided the following parameter set: C–N = 1.33 ± 0.02 Å, C–Cl = 1.68 ± 0.03 Å, and N–C–N angle = 125 ± 3° (apparently assuming that the triazine ring is a regular hexagon, which has been shown to be incorrect).<sup>14-16</sup> We report this earlier work because these results were used in the analysis of the crystal vibrational spectrum provided by Thomas *et al.*,<sup>19</sup> against which we compare our results.

There is good agreement between the calculated and experimental structural parameters for cyanuric chloride (Table 1). The MP2/6-311+G\* and DFT/cc-pVTZ predictions of all structural parameters are within 1% of experiment. Both methods predict C–N bond distances in the cyanogen chloride molecule that are within 2% or less of the experimental gas-phase values.<sup>17</sup> Both methods predict C–Cl bond distances that are within 0.5% of experiment.<sup>17</sup>

Structures obtained from MP2 are qualitatively similar to those predicted by DFT for the transition state for reaction I, the dimer, and the transition state for dimer formation in reaction II. The structures of the transition state for reaction I and the dimer are very similar to those of the *sym*-triazine system.<sup>5,6</sup> We did not look for the transition state for formation of the dimer from the monomers in the *sym*-triazine study since we had eliminated that reaction as the low-energy mechanism after comparing relative energetics of the dimer minimum with the transition state for 3-fold concerted reaction. It was necessary to determine the transition state for dimer formation from two ClCN, since the energy of the stable dimer (*i.e.*, Cl<sub>2</sub>C<sub>2</sub>N<sub>2</sub> + ClCN) lies below or is only slightly higher than the transition state I. The structure of this species is nonplanar although the

**TABLE 1: Geometric Parameters for Critical Points on the Cyanuric Chloride Potential Energy Surface**

parameter	MP2		B3LYP			exptl (ref 13–16)
	6-31G*	6-311+G*	6-31G*	6-311+G*	cc-pVTZ	
Cyanuric Chloride						
C1N2	1.3353	1.3338	1.3304	1.3270	1.3247	1.325
C3N2	1.3353	1.3338	1.3304	1.3270	1.3247	1.325
C3N4	1.3353	1.3338	1.3302	1.3269	1.3247	1.325
C5N4	1.3353	1.3338	1.3302	1.3269	1.3246	1.325
C5N6	1.3353	1.3338	1.3303	1.3270	1.3246	1.325
C5C17	1.7159	1.7119	1.7331	1.7309	1.7280	1.703
C3C18	1.7159	1.7119	1.7329	1.7308	1.7280	1.703
C1C19	1.7159	1.7119	1.7328	1.7307	1.7280	1.703
C3N2C1	113.15	113.16	113.14	113.40	113.42	112.7
N4C3N2	126.85	126.84	126.85	126.59	126.57	127.4
C5N4C3	113.15	113.16	113.16	113.42	113.44	112.7
N6C5N4	126.85	126.84	126.85	126.59	126.56	127.4
N4C5C17	116.58	116.58	116.55	116.69	116.72	
N2C3C18	116.58	116.58	116.60	116.72	116.73	
N6C1C19	116.58	116.58	116.57	116.70	116.70	
Transition State (I)						
C1N2	1.2078	1.2034	1.1863	1.1806	1.1776	
C3N2	1.9567	1.9523	2.0331	2.0144	2.0091	
C3N4	1.2078	1.2034	1.1863	1.1806	1.1777	
C5N4	1.9567	1.9522	2.0342	2.0155	2.0079	
C5N6	1.2078	1.2034	1.1864	1.1806	1.1777	
C5C17	1.6697	1.6661	1.6759	1.6737	1.6696	
C3C18	1.6697	1.6661	1.6760	1.6737	1.6694	
C1C19	1.6697	1.6661	1.6758	1.6737	1.6693	
C3N2C1	119.43	119.98	123.09	123.34	123.34	
N4C3N2	120.57	120.02	116.93	116.68	116.66	
C5N4C3	119.43	119.98	123.10	123.32	123.38	
N6C5N4	120.57	120.02	116.92	116.67	116.67	
N6C5C17	139.75	140.32	144.63	144.22	144.43	
N4C3C18	139.75	140.32	144.58	144.18	144.45	
N2C1C19	139.75	140.32	144.58	144.18	144.51	
CICN						
CN	1.1844	1.1787	1.1633	1.1556	1.1533	1.160 ± 0.007 <sup>a</sup>
CCl	1.6380	1.6341	1.6455	1.6408	1.6368	1.629 ± 0.006 <sup>a</sup>
CICN	180.00	180.00	180.00	180.00	180.00	180.00
Dimer						
C1N2	1.2900	1.2897	1.2857	1.2832	1.2807	
C3N2	1.5242	1.5220	1.5143	1.5101	1.5081	
C3N4	1.2900	1.2897	1.2857	1.2832	1.2807	
C3H8	1.6823	1.6755	1.6959	1.6898	1.6866	
C1H9	1.6823	1.6755	1.6959	1.6898	1.6866	
C3N2C1	76.79	77.28	77.40	77.85	77.81	
N4C3N2	103.22	102.72	102.60	102.15	102.19	
N4C3C18	132.00	132.21	131.62	131.65	131.69	
N2C1C19	132.00	132.21	131.62	131.65	131.69	
Transition State (II)						
C1N2	1.2407	1.2378	1.2207	1.2146	1.2114	
C3N2	1.8892	1.8853	1.9122	1.8993	1.8972	
C3N4	1.2408	1.2377	1.2206	1.2146	1.2114	
C3C18	1.7064	1.6989	1.7241	1.7182	1.7137	
C1C19	1.7064	1.6992	1.7250	1.7185	1.7139	
N4C3N2	116.43	115.17	113.00	112.23	111.95	
N4C3C18	138.85	139.51	140.91	141.03	141.66	
N2C1C19	138.85	139.47	140.76	141.00	141.65	
N4C3N2C4	−150.43	−149.89	−143.02	−144.94	−145.81	
C18C3N4C1	155.76	155.37	153.61	154.00	154.52	
C19C1N2C3	155.77	155.42	153.84	154.03	154.48	
(CICN) <sub>3</sub>						
C1N2	1.1841	1.1787	1.1630	1.1555	1.1532	
C3N2	3.1150	3.1067	3.3944	3.5337	3.6131	
C3N4	1.1841	1.1786	1.1630	1.1555	1.1532	
C5N4	3.1169	3.1088	3.3462	3.5068	3.5711	
C5N6	1.1841	1.1787	1.1630	1.1555	1.1532	
C5C17	1.6342	1.6305	1.6420	1.6370	1.6329	
C3C18	1.6342	1.6305	1.6417	1.6370	1.6328	
C1C19	1.6343	1.6305	1.6419	1.6371	1.6329	
N6C5C17	177.70	178.55	178.67	179.26	179.28	
N2C18C3	67.43	68.16	72.77	76.77	79.45	
C18N2C1	170.14	170.34	164.77	162.25	159.87	
N2C18	3.3525	3.3199	3.4969	3.5287	3.5359	

<sup>a</sup> Reference 17. Values are  $r_e$ .

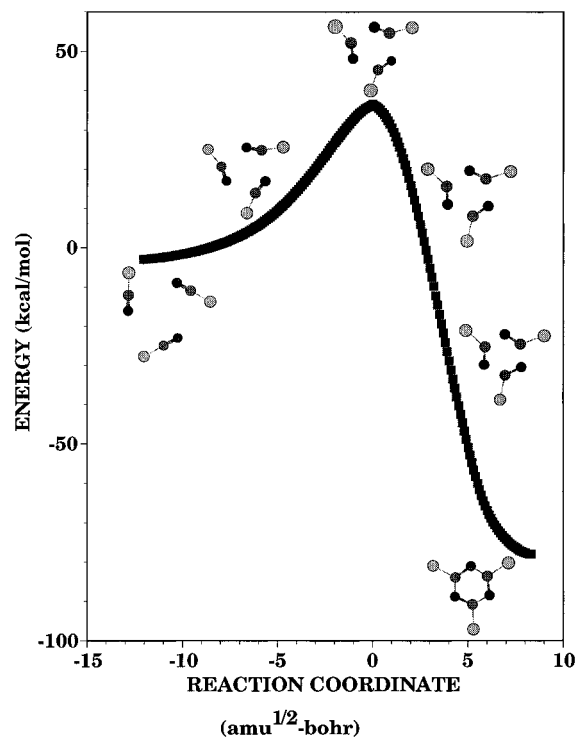


**Figure 2.** B3LYP/6-31G\* energies along the reaction path for reaction I. The stable and transition state structures and three other structures along the reaction path have been shown to enable the reader to visualize the mechanism of concerted triple association and dissociation. The  $(\text{CICN})_3$  cluster is illustrated in the far-left portion of the figure. The cyanuric chloride molecule is represented by the far-right structure of the figure.

stable dimer is planar. The optimized structure of the  $(\text{CICN})_3$  cluster is cyclic and has a  $C_3$  axis of rotation.

**Intrinsic Reaction Coordinate Calculations.** Energies and structures along the reaction path for concerted triple association determined from B3LYP/6-31G\* IRC calculations are shown in Figure 2. The energies are relative to 3CICN. Negative values of the reaction coordinate correspond to the  $(\text{CICN})_3$  cluster region of the PES and positive values along the reaction coordinate correspond to the cyanuric chloride region of the PES. The reaction path coordinate value 0.0 corresponds to the transition state connecting the  $(\text{CICN})_3$  cluster and cyanuric chloride minima. The  $C_3$  axis of rotation of the structures, while not imposed in the calculations, is maintained all along the reaction path.

The greatest difference in structural parameters between the cyanuric chloride and *sym*-triazine systems is in the  $(\text{XCN})_3$  cluster, X = Cl, H. However, the structures at the transition state for the concerted triple association of CICN to form cyanuric chloride are very similar to those for *sym*-triazine formation: The CN1 and C–Cl bonds have almost the same values as the isolated monomer. Also, the CICN angle ( $144^\circ$ ) is closer to the cyanuric chloride value ( $122^\circ$ ) than the monomer/cluster value ( $180^\circ$ ). The large difference in the XCN angle between the transition state and the XCN monomers was used to explain the substantial vibrational excitation of the bending vibration in the HCN product upon decomposition of *sym*-triazine.<sup>20</sup> Since the features along the IRC for this system are similar to that of the *sym*-triazine system, it is reasonable to predict that vibrationally hot CICN product molecules, preferentially excited in the bending mode, would be observed upon photodissociation of cyanuric chloride.

**Frequencies.** Table 2 lists the harmonic vibrational frequencies of the critical points for reactions I and II calculated using

the *ab initio* and DFT methods and the basis sets mentioned in the previous sections. We present the frequencies of the smaller 6-31G\* basis due to the use of only this basis in all of the IRC calculations.

The most complete vibrational analysis for this system was performed by Thomas *et al.*<sup>19</sup> They reported the single-crystal infrared and Raman spectra for cyanuric chloride at 298 and 77 K and made complete assignments for all fundamentals. Additionally, they performed a normal coordinate analysis using a modified valence force field model and assumed that the triazine ring of the cyanuric chloride is a regular hexagon with all angles equal to  $120^\circ$ . They also assumed the C–N and C–Cl bond lengths given by Akimoto.<sup>13</sup> A fit of this model to the observed frequencies resulted in a set of frequencies and corresponding eigenvectors for the normal modes of cyanuric chloride (Figure 9 of ref 19). Wilson later analyzed the gas phase spectrum of cyanuric chloride<sup>21</sup> and changed only a few of the vibrational assignments of Thomas *et al.*<sup>19</sup> He reports that, with the exception of  $\nu_{11}$  ( $749\text{ cm}^{-1}$  in gas phase,  $795\text{ cm}^{-1}$  in the solid), the gas-phase spectrum of cyanuric chloride is very similar to that of the condensed phase. We were able to match all calculated vibrational modes of the cyanuric chloride to experimental assignments through visual inspection of the eigenvectors when compared to those illustrated in Figure 9 of ref 19. Calculated vibrational frequencies of cyanuric chloride are within  $100\text{ cm}^{-1}$  of the experimental frequencies with the exception of modes denoted  $\nu_4$  and  $\nu_5$  in ref 19 (modes 16 and 9 here). In the gas phase, these  $A_2'$  modes are inactive and not observed; however, in the solid phase, data for these modes were available and resulted in the assignment of bands at  $1590$  and  $610\text{ cm}^{-1}$  to  $\nu_4$  and  $\nu_5$ , respectively. For the methods used in this study, the calculated frequencies corresponding to  $\nu_4$  and  $\nu_5$  differ from experiment by  $\sim 400$  and  $\sim 110\text{ cm}^{-1}$ , respectively. A similar large discrepancy between theory and experiment for these two  $A_2'$  modes for *sym*-triazine was found as well.<sup>5,6</sup> The predicted frequencies of CICN agree to within  $100\text{ cm}^{-1}$  of experiment<sup>17</sup> for all methods and basis sets. There are no measured vibrational spectra for the other critical points.

**Vibrational Coupling.** In our previous study, we used a method of projecting the vibrational eigenvectors of *sym*-triazine and the symmetric  $(\text{HCN})_3$  cluster onto the reaction path for the concerted triple-association reaction.<sup>5</sup> Our premise in doing so was based on studies that indicate a correlation between the magnitude of the projection of a vibration onto the reaction coordinate and the coupling of that mode with the reaction path.<sup>22,23</sup> For modes that project strongly onto the reaction coordinate, we concluded that these vibrations are possible efficient energy transfer routes between the molecules and the reaction coordinate.

In this study, we provide a similar analysis of the vibrational modes. As detailed in our previous work,<sup>5</sup> we calculated local normal modes<sup>24</sup> for points along the reaction path for reaction I at the B3LYP/6-31G\* level and projected out the infinitesimal translations and rotations, leaving  $3N-7$  bound vibrational modes of the molecule plus the eigenvector corresponding to the direction along the reaction path.<sup>24</sup> We then projected the eigenvectors corresponding to the harmonic vibrational frequencies of equilibrium cyanuric chloride and the  $(\text{CICN})_3$  cluster onto the eigenvector associated with the direction along the reaction path for selected reaction coordinate values. The results of these projections onto the reaction path eigenvectors are shown in Figures 3 and 4, respectively. Only those modes that have projections greater than 0.05 are shown in these figures. There are five vibrational modes of cyanuric chloride that project

**TABLE 2: Harmonic Vibrational Frequencies (cm<sup>-1</sup>)**

mode	MP2		B3LYP			exptl	mode	MP2		B3LYP		
	6-31G*	6-311+G*	6-31G*	6-311+G	cc-pVTZ			6-31G*	6-311+G*	6-31G*	6-311+G	cc-pVTZ
Cyanuric Chloride						(CICN) <sub>3</sub>						
1	142	138	139	139	140	156 <sup>b</sup>	1	14	13	8	17	13
2	168	156	165	163	165	178 <sup>b</sup>	2	14	14	16	20	18
3	168	156	166	164	167	178 <sup>b</sup>	3	24	28	24	24	20
4	213	211	208	208	207	216 <sup>b</sup>	4	54	56	33	26	22
5	213	211	209	208	208	216 <sup>b</sup>	5	54	56	34	28	25
6	411	413	399	398	396	408 <sup>b</sup>	6	63	66	50	38	34
7	474	476	463	464	461	474, <sup>b</sup> 461 <sup>c</sup>	7	63	66	51	47	48
8	474	476	463	464	462	474, <sup>b</sup> 461 <sup>c</sup>	8	73	78	54	48	49
9	509	505	505	505	501	610 <sup>b</sup>	9	98	99	62	53	51
10	646	606	655	651	667	652 <sup>b</sup>	10	349	346	395	390	407
11	646	606	656	651	667	652 <sup>b</sup>	11	351	346	396	391	408
12	796	749	811	815	820	795, <sup>b</sup> 749 <sup>c</sup>	12	351	348	396	394	411
13	877	880	859	859	854	849 <sup>b</sup>	13	357	354	399	397	412
14	877	880	860	860	854	849 <sup>b</sup>	14	357	354	400	397	412
15	995	998	989	993	987	977 <sup>b</sup>	15	361	358	402	399	413
16	1284	1265	1227	1201	1197	1590, <sup>b</sup> 1595 <sup>c</sup>	16	763	764	748	746	749
17	1308	1298	1287	1278	1279	1297 <sup>b</sup>	17	763	764	748	746	749
18	1322	1311	1301	1292	1290	1260 <sup>b</sup>	18	763	764	749	747	749
19	1322	1311	1301	1293	1290	1260 <sup>b</sup>	19	2159	2138	2328	2310	2310
20	1573	1559	1550	1539	1534	1500 <sup>b</sup>	20	2159	2138	2328	2310	2310
21	1573	1559	1550	1539	1534	1500 <sup>b</sup>	21	2159	2138	2329	2311	2311
CICN						Dimer						
1	349	346	392	392	405	378 <sup>d</sup>	1	97	94	102	104	105
2	349	346	392	392	405	378 <sup>d</sup>	2	223	223	211	211	211
3	755	757	741	740	742	744 <sup>d</sup>	3	369	370	361	361	359
4	2154	2135	2326	2310	2311	2216 <sup>d</sup>	4	484	472	469	472	469
TS <sup>a</sup> (I)						TS(II)						
1	584i	563i	519i	529i	539i		5	487	483	495	500	513
2	71	51	64	69	65		6	637	642	614	617	615
3	71	51	65	70	66		7	658	654	678	689	691
4	77	65	69	72	69		8	904	903	916	908	907
5	144	144	123	121	124		9	964	969	947	948	941
6	144	144	124	122	124		10	1137	1136	1086	1081	1074
7	264	264	225	227	227		11	1645	1621	1582	1562	1559
8	264	264	225	227	227		12	1664	1640	1641	1623	1620
9	304	303	281	284	283		1	595i	598i	519i	555i	570i
10	456	432	440	441	441		2	81	79	88	83	79
11	456	432	441	441	441		3	274	272	238	236	236
12	485	459	447	454	460		4	326	323	303	303	300
13	487	482	448	454	461		5	458	458	435	434	438
14	487	482	479	489	495		6	502	494	453	452	446
15	517	521	510	521	522		7	538	533	499	496	496
16	732	735	698	694	693		8	547	548	508	498	499
17	811	809	762	758	758		9	720	715	612	602	599
18	811	809	762	758	758		10	842	825	731	708	698
19	1958	1930	2022	1990	1993		11	1724	1698	1800	1781	1782
20	2001	1977	2109	2085	2087		12	1950	1911	1924	1911	1914
21	2001	1977	2110	2086	2087							

<sup>a</sup> TS = transition state. <sup>b</sup> Reference 19. <sup>c</sup> Reference 21. <sup>d</sup> Reference 17.

strongly onto the reaction path for (I); their atomic motions are illustrated in Figure 3. All of these motions exhibit a 3-fold symmetric axis of rotation perpendicular to the plane of the triazine ring, and three of them (399, 989, and 1227 cm<sup>-1</sup>) are similar to the *sym*-triazine vibrational modes that project strongly onto reaction I. Cyanuric chloride has no analog to the remaining *sym*-triazine mode that projects weakly onto the reaction coordinate for reaction I.

There are three vibrational modes for the (CICN)<sub>3</sub> cluster that project strongly onto the reaction path, and three additional vibrational modes that project less strongly. The atomic motions corresponding to these normal modes of vibration are illustrated in Figure 4. A comparison of these modes with those of the (HCN)<sub>3</sub> cluster that project onto the *sym*-triazine reaction coordinate<sup>5,6</sup> cannot be performed due to the significant differences in the structure of the clusters of the two systems.

As in our previous study, we conclude that the vibrations that project onto the reaction coordinate indicate the most likely routes through which reaction energy distributed in either of these species can transfer efficiently to the reaction coordinate for (I).

**Energetics.** Absolute energies of critical points on the cyanuric chloride PES are given in Table 3. The heats of reaction and the energies of critical points relative to three isolated CICN molecules are also given in Table 3. All relative energies discussed in this section have been corrected for zero-point energies.

For both methods and all basis sets other than QCISD(T)//MP2/6-311+G\*, the minimum corresponding to the dimer + CICN is lower in energy than that of the barrier to concerted triple association. The QCISD(T)//MP2/6-311+G\* results predict that the dimer + CICN minimum is only 1 kcal/mol higher in energy than that of the barrier to concerted triple

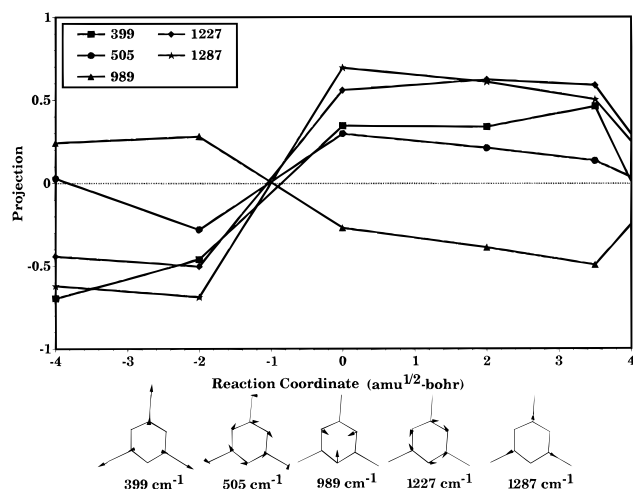


**Figure 3.** Projection of B3LYP/6-31G\* eigenvectors corresponding to harmonic vibrational frequencies of cyanuric chloride onto eigenvectors that correspond to the direction along the reaction path for the concerted triple-association reaction (reaction I). Eigenvectors with projections greater than 0.05 are illustrated, and labeled with the corresponding B3LYP/6-31G\* harmonic vibrational frequency (in  $\text{cm}^{-1}$ ). The vibrational modes are illustrated at the bottom of the figure.

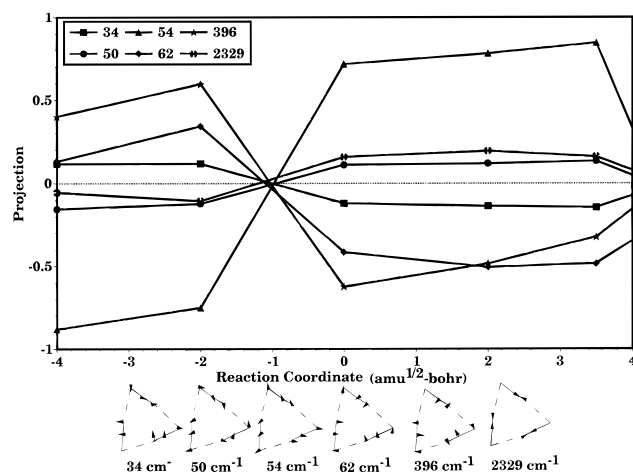


**Figure 4.** Projection of B3LYP/6-31G\* eigenvectors corresponding to harmonic vibrational frequencies of the  $(\text{CICN})_3$  cluster onto eigenvectors that correspond to the direction along the reaction path for the concerted triple association reaction (reaction I). Eigenvectors with projections greater than 0.05 are illustrated and are labeled with the corresponding B3LYP/6-31G\* harmonic vibrational frequency (in  $\text{cm}^{-1}$ ). The vibrational modes are illustrated at the bottom of the figure.

association. This is different than the *sym*-triazine system, in which all methods predicted that the dimer + HCN minimum was higher in energy than the barrier to concerted triple association.<sup>5,6</sup> Since our primary goal is to determine the lowest-energy pathway to formation of cyanuric chloride, we located the saddle point leading to formation of the dimer from CICN to determine if it was lower in energy than that of the barrier to (I). At all levels and using all basis sets, the barrier to formation of the dimer is significantly higher in energy than that of the barrier to triple concerted association. The DFT/cc-pVTZ barrier to formation of the dimer is 63.4 kcal/mol; the DFT/cc-pVTZ barrier to concerted triple association is 42.9 kcal/mol. The QCISD(T)/MP2/6-311+G\* barrier for concerted triple association is 41.0 kcal/mol. The QCISD(T)/MP2/6-311+G\* barrier to formation of the dimer is 76.7 kcal/mol.

The free energy of activation for these associations include the effect of entropy, which could be quite important in these reactions. We calculated the free energies of activation for reactions I and II at the B3LYP/cc-pVTZ level. For reaction I,

we calculated the free energy of activation from the cluster minimum. For reaction II, we calculated the free energy of activation from the CICN reactants. The free energies of activation for reactions I and II are 53.4 and 72.6 kcal/mol, which are 7.6 and 9.2 kcal/mol higher in energy than the respective zero-point-corrected barriers. We also calculated the free energy of activation for reaction I from the three isolated CICN reactants. The free energy of activation in reaction I at the B3LYP/cc-pVTZ level from the isolated molecules is 61.8 kcal/mol, which is  $\sim 19$  kcal/mol higher than the energy of the zero-point-corrected barrier. It is worth noting the reduction in the entropic contribution to the free energy of activation by the formation of the cyclic cluster, which significantly increases the probability of this reaction path.

Since the barrier for the formation of the dimer is so much higher than that of the triple concerted association reaction, this mechanism was eliminated as the lower-energy path for formation of cyanuric chloride. Therefore, we did not search for the transition state for addition of a CICN molecule to the dimer to form cyanuric chloride. As in the *sym*-triazine system, the lower-energy pathway to formation of cyanuric chloride is the concerted triple association. Thermal activation barriers for I or its reverse (concerted triple dissociation) have not been measured. Therefore, we cannot gauge the accuracy of these barrier heights. For the analogous system, *sym*-triazine, the B3LYP/cc-pVTZ barriers were within 6 and 2 kcal/mol of the QCISD(T)/MP2/cc-pVTZ predictions for the forward and reverse of I, respectively.

Both methods show a significant heat of reaction ( $T = 298$  K) for formation of cyanuric chloride (Table 3). The DFT/cc-pVTZ value is  $-63.4$  kcal/mol and the QCISD(T)/MP2/6-311+G\* prediction is  $-61.2$  kcal/mol. We showed in our previous study<sup>6</sup> on *sym*-triazine that the B3LYP/cc-pVTZ predictions were within 1.1 kcal/mol agreement with experimental measurements of the reaction enthalpy, which was significantly better than QCISD(T)/MP2/cc-pVTZ predictions. If this trend is maintained for the cyanuric chloride system, the heat of reaction for formation of cyanuric chloride is approximately  $-63$  kcal/mol.

As in the *sym*-triazine system,<sup>5,6</sup> reaction path calculations indicate that the weakly-bound cyclic  $(\text{CICN})_3$  cluster is a reaction intermediate to the formation of cyanuric chloride. Our DFT/cc-pVTZ and QCISD(T)/MP2/6-311+G\* calculations indicate that this species is lower in energy than isolated monomers by 2.9 and 8 kcal/mol, respectively.

These calculations correspond to gas-phase reactions, whereas the XCN ( $X = \text{H}$  and  $\text{Cl}$ ) in the munitions described in the Introduction are compressed to the liquid state. It is well-known that reaction barriers can be affected when in solution phase.<sup>25,26</sup> Therefore, the barriers to association calculated in this study could be an upper limit for reactions of CICN in aged munitions. Also the cluster is a pre-reaction intermediate on the concerted triple-association pathway and has an arrangement of atoms that is favorable to concerted triple association. This could significantly reduce the entropic hindrance to such an unusual association reaction. Once the barrier is crossed, our calculations indicate that there is substantial energy ( $\sim 100$  kcal/mol assuming gas-phase barriers) available to the translational or internal modes of the product. This amount of energy is sufficient to initiate additional reaction. A translationally "hot" cyanuric chloride molecule in the liquid state could easily transfer energy through collisions with adjacent species (including clusters) in the liquid. The large reaction exothermicity for cyanuric chloride formation and other features of the PES lend

**TABLE 3: Heats of Reaction, Absolute, Zero-Point, and Zero-Point-Corrected Relative Energies on the Cyanuric Chloride PES**

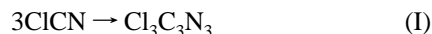
species	MP2		QCISD(T)//MP2		B3LYP		
	6-31G*	6-311+G*	6-31G*	6-311+G*	6-31G*	6-311+G*	cc-pVTZ
Absolute Energies (hartrees)							
3CICN	-1656.528659	-1656.742607	-1656.620474	-1656.834437	-1659.024875	-1659.196029	-1659.251138
TS (I)	-1656.465855	-1656.685078	-1656.552678	-1656.772563	-1658.966562	-1659.133727	-1659.184605
Cl <sub>3</sub> C <sub>3</sub> N <sub>3</sub>	-1656.630890	-1656.845927	-1656.72221	-1656.939247	-1659.149350	-1659.307506	-1659.357780
(CICN) <sub>3</sub>	-1656.539456	-1656.757453	-1656.629530	-1656.848318	-1659.030670	-1659.201592	-1659.256393
dimer+CICN	-1656.476237	-1656.692887	-1656.574029	-1656.772103	-1658.988540	-1659.153089	-1659.204679
TS <sup>a</sup> (II)	-1656.423892	-1656.642264	-1656.514318	-1656.713778	-1658.930450	-1659.096855	-1659.149446
Zero-Point Energies (kcal/mol)							
3CICN	15.5	15.4	15.5	15.4	16.5	16.4	16.6
TS (I)	17.9	17.6	17.9	17.6	17.7	17.7	17.7
Cl <sub>3</sub> C <sub>3</sub> N <sub>3</sub>	22.9	22.5	22.9	22.5	22.5	22.4	22.4
(CICN) <sub>3</sub>	16.2	16.1	16.2	16.1	17.1	16.9	17.0
dimer+CICN	18.4	18.3	18.4	18.3	18.5	18.4	18.5
TS (II)	16.5	16.4	16.5	16.4	16.4	16.2	16.2
Zero-Point-Corrected Relative Energies (kcal/mol)							
3CICN	0.0	0.0	0.0	0.0	0.0	0.0	0.0
TS (I)	41.8	38.3	44.9	41.0	37.8	40.4	42.9
Cl <sub>3</sub> C <sub>3</sub> N <sub>3</sub>	-56.8	-57.7	-56.4	-58.7	-72.1	-64.0	-61.1
(CICN) <sub>3</sub>	-6.1	-8.6	-5.0	-8.0	-3.0	-3.0	-2.9
dimer+CICN	35.8	34.1	32.0	42.0	24.8	28.9	31.1
TS (II)	66.7	64.0	67.6	76.7	59.2	62.0	63.4
$\Delta H (T = 298 \text{ K})$ (kcal/mol)							
	-60.0	-60.2	-59.6	-61.2	-74.4	-66.3	-63.4

<sup>a</sup> TS = transition state.

support to the suggestion that acceleration of this reaction could contribute to the initiation of explosions of aged containers of CICN.<sup>1</sup>

#### IV. Conclusions

We have presented *ab initio* and DFT calculations of formation reactions of cyanuric chloride from isolated CICN. Two pathways were examined: A concerted triple association reaction



and a stepwise association reaction, in which a dimer is first formed followed by addition of another CICN to form cyanuric chloride



Critical points associated with these two reactions were located through MP2 and DFT (B3LYP) geometry optimizations using basis sets of varying sizes and were characterized through normal mode analyses. Energy refinements of the MP2 calculations were done at the QCISD(T) level. Predicted structures were in reasonable agreement with experiment, where available. As in previously reported calculations on the hydrogen analog of this system,<sup>5,6</sup> the geometry of cyanuric chloride is described extremely well at the DFT level with all three basis sets, which suggests accurate geometries are available without requiring large basis sets or computationally expensive perturbation techniques. The MP2 and DFT frequencies are within  $\sim 100 \text{ cm}^{-1}$  of their corresponding experimental values where available.

The zero-point-corrected DFT/cc-pVTZ energy barrier for II is 63.4 kcal/mol; the DFT/cc-pVTZ energy barrier for (I) is 42.9 kcal/mol. QCISD(T)//MP2/6-311+G\* barriers are 76.7 kcal/mol for reaction II and 41.0 kcal/mol for reaction I. These results indicate that the lower-energy pathway to formation of cyanuric chloride from isolated monomer molecules is through the concerted triple association reaction. Additionally, MP2 and

B3LYP intrinsic reaction coordinate (IRC) calculations for reaction I resulted in the location of a local minimum on the potential energy surface that corresponds to a weakly-bound cyclic (CICN)<sub>3</sub> cluster.

The (CICN)<sub>3</sub> cluster, whose hydrogen analog was seen experimentally and theoretically determined for the *sym*-triazine system,<sup>5,6</sup> is a prereaction intermediate leading to the formation of cyanuric chloride. Its energy relative to isolated CICN is within the range of  $-2.9$  to  $-8.0$  kcal/mol. The arrangement of the atoms in this cluster removes significant steric hindrance to the concerted triple association reaction. Reaction energy appropriately imparted to the cluster would result in the concerted triple association to form cyanuric chloride.

The heat of reaction for formation of cyanuric chloride ( $T = 298 \text{ K}$ ) from the B3LYP/cc-pVTZ calculations is  $-63.4$  kcal/mol, in close agreement with the QCISD(T)//MP2/6-311+G\* prediction ( $-61.2$  kcal/mol). This heat of reaction, coupled with the barrier to formation of cyanuric chloride from 3CICN, indicate that upon traversing the association barrier,  $\sim 100$  kcal/mol energy is available to the product and surroundings.

We also projected the vibrational eigenvectors of cyanuric chloride and the (CICN)<sub>3</sub> cluster onto the eigenvector associated with the direction of the reaction coordinate at various points along the reaction path for the concerted reaction. For points all along the reaction path, including the transition state, five vibrational modes of cyanuric chloride and six vibrational modes of the (CICN)<sub>3</sub> cluster project onto the reaction path. These projections indicate that certain vibrational modes of cyanuric chloride and the (CICN)<sub>3</sub> cluster are coupled to the reaction coordinate, suggesting efficient pathways through which reaction energy of either stable species can couple with the reaction path for the concerted association/decomposition reactions. The energy released upon traversing the barrier to formation of cyanuric chloride is sufficient to initiate additional reaction. The large energy release and the prereaction cluster intermediate support the suggestion that acceleration of polymerization reactions of CICN could be contributing factors leading to explosions of aged containers of CICN.

**Acknowledgment.** This work was supported by the Program Manager Non-Stockpile Chemical Materiel, U.S. Army Chemical Demilitarization and Remediation Activity. All calculations were performed on the Silicon Graphics Power Challenge Array located at the DOD High Performance Computing Site, U.S. Army Research Laboratory, Aberdeen, Maryland.

## References and Notes

- (1) Aaron, H. S.; Burke, L. A.; Jensen, J. O.; Krishnan, P. N.; Vlahacos, C. P.; Chabalowski, C. F.; McNesby, K. L.; McQuaid, M. J.; Pai, S. V.; Rice, B. M. Technical Report No. ARL-TR-1097; U.S. Army Research Laboratory: Aberdeen Proving Ground, MD, June, 1996.
- (2) Migridichian, V. *The Chemistry of Organic Cyanogen Compounds*; Reinhold Publishing Co.: New York, 1947.
- (3) Enders, E. Production of Cyanogen Chloride Together with Cyanuric Chloride and Tetrameric Cyanogen Chloride. U.S. Patent 3,666,427, May 30, 1972 [*Chem. Abstr.* **1972**, 77, 64173].
- (4) Bretherick, L. *Bretherick's Handbook of Reactive Chemical Hazards*, 4th ed.; Butterworths and Co.: London, England, 1990.
- (5) Pai, S. V.; Chabalowski, C. F.; Rice, B. M. *J. Phys. Chem.* **1996**, *100*, 5681.
- (6) Pai, S. V.; Chabalowski, C. F.; Rice, B. M. *J. Phys. Chem.* **1996**, *100*, 15368.
- (7) Frisch, M. J.; Trucks, G. W.; Schlegel, H. B.; Gill, P. M. W.; Johnson, B. G.; Robb, M. A.; Cheeseman, J. R.; Keith, T.; Petersson, G. A.; Montgomery, J. A.; Raghavachari, K.; Al-Laham, M. A.; Zakrzewski, V. G.; Ortiz, J. V.; Foresman, J. B.; Cioslowski, J.; Stefanov, B. B.; Nanayakkara, A.; Challacombe, M.; Peng, C. Y.; Ayala, P. Y.; Chen, W.; Wong, M. W.; Andres, J. L.; Replogle, E. S.; Gomperts, R.; Martin, R. L.; Fox, D. J.; Binkley, J. S.; Defrees, D. J.; Baker, J.; Stewart, J. P.; Head-Gordon, M.; Gonzalez, C.; Pople, J. A. *Gaussian 94*, Revision B.1; Gaussian, Inc., Pittsburgh, PA, 1995.
- (8) Hehre, W. J.; Ditchfield, R.; Pople, J. A. *J. Chem. Phys.* **1972**, *56*, 2257. Hariharan, P. C.; Pople, J. A. *Theor. Chim. Acta.* **1973**, *28*, 213. Gordon, M. S. *Chem. Phys. Lett.* **1980**, *76*, 163.
- (9) McLean, A. D.; Chandler, G. S. *J. Chem. Phys.* **1980**, *72*, 5639. Krishnan, R.; Binkley, J. S.; Seeger, R.; Pople, J. A. *J. Chem. Phys.* **1980**, *72*, 650.
- (10) Woon, D. E.; Dunning, T. H., Jr. *J. Chem. Phys.* **1993**, *98*, 1358. Kendall, R. A.; Dunning, T. H., Jr.; Harrison, R. J. *J. Chem. Phys.* **1992**, *96*, 6796. Dunning, T. H., Jr. *J. Chem. Phys.* **1989**, *90*, 1007.
- (11) Becke, A. D. *J. Chem. Phys.* **1993**, *98*, 5648.
- (12) Lee, C.; Yang, W.; Parr, R. G. *Phys. Rev. B.* **1988**, *37*, 785. Miehlich, B.; Savin, A.; Stoll, H.; Preuss, H. *Chem. Phys. Lett.* **1989**, *157*, 200.
- (13) Akimoto, Y. *Bull. Chem. Soc. Jpn.* **1955**, *28*, 1.
- (14) Pascal, R. A., Jr.; Ho, D. M. *Tetrahedron Lett.* **1992**, *33*, 4707.
- (15) Xu, K.; Ho, D. M.; Pascal, R. A., Jr. *J. Am. Chem. Soc.* **1994**, *116*, 105.
- (16) Maginn, S. J.; Compton, R. G.; Harding, M. S.; Brennan, C. M.; Docherty, R. *Tetrahedron Lett.* **1993**, *34*, 4349.
- (17) Lafferty, W. J.; Lide, D. R.; Toth, R. A. *J. Chem. Phys.* **1965**, *43*, 2063.
- (18) Lancaster, J. E.; Stoicheff, B. P. *Can. J. Phys.* **1956**, *34*, 1016.
- (19) Thomas, D. M.; Bates, J. B.; Bandy, A.; Lippincott, E. R. *J. Chem. Phys.* **1970**, *53*, 3698.
- (20) Ondrey, G. S.; Bersohn, R. *J. Chem. Phys.* **1984**, *81*, 4517.
- (21) Wilson, H. W. *J. Chem. Phys.* **1973**, *58*, 2663.
- (22) Waite, B. A.; Miller, W. H. *J. Chem. Phys.* **1981**, *74*, 3910.
- (23) Rice, B. M.; Grosh, J.; Thompson, D. L. *J. Chem. Phys.* **1995**, *102*, 8790.
- (24) Miller, W. H.; Handy, N. C.; Adams, J. E. *J. Chem. Phys.* **1980**, *72*, 99.
- (25) Hynes, J. T. *Annu. Rev. of Phys. Chem.* **1985**, *36*, 573.
- (26) Hynes, J. T. *Nature* **1994**, *369*, 439.